DOI: 10.1002/chem.201000669

# A Computational Study of Rhodium Pincer Complexes with Classical and Nonclassical Hydride Centres as Catalysts for the Hydroamination of Ethylene with Ammonia

**Andreas Uhe, Markus Hölscher,* and Walter Leitner*[a]**

**Abstract:** The catalytic hydroamination of ethylene with ammonia was investigated by means of density functional theory (DFT) calculations. An initial computational screening of key reaction steps (C–N bond formation, N–H bond cleavage), which are assumed to be part of a catalytic cycle, was carried out for complexes with the [M(L)]-complex fragment (M = Rh, Ir; L = NCN, PCP; NCN = 2,5-bis(dimethylaminomethyl)benzene, PCP = 2,5-bis-(dimethylphosphanylmethyl)benzene). Based on the evaluation of activation barriers, this screening showed the rhodium compound with the NCN ligand to be the most promising catalyst system. A detailed investigation was carried out starting with the hypothetical catalyst precursor [Rh-(NCN)$(H)_2(H_2)$] (**1**). A variety of activation pathways to yield the catalytically active species [Rh(NCN)(H)$(NH_2)$] (**5**), as well as [Rh(NCN)$(C_2H_5)(NH_2)$] (**17**), were identified. With **5** and **17** several closed catalytic cycles could be calculated. One of the calculated cycles is favoured kinetically and bond-forming events have activation barriers low enough to be put into practice. The calculations also show that for experimental realisation the synthesis of **1** is not necessary, as the synthesis of **17** would establish an active catalyst directly without the need for activation. Oligomerisation of ethylene would be possible in principle and would be expected as a competitive side reaction. Accordingly not only ethylamine would be observed in an experimental system, as amines with longer carbon chains also can be formed.

**Keywords:** density functional calculations · homogeneous catalysis · hydroamination · pincer complexes · rhodium

## Introduction

The hydroamination, that is, the direct addition of an amine (or ammonia) to a C=C bond is a powerful and atom-efficient reaction for the formation of amines (Scheme 1).

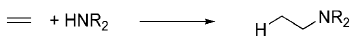


Scheme 1. Hydroamination of olefins (R = H, Alkyl).

The addition of amines to C≡C bonds yields enamines. Both product classes are highly valuable building blocks in fine chemical synthesis, and particularly amines have an important relevance for bulk chemical syntheses. Although hydroamination is allowed thermodynamically, the activation barrier for the uncatalysed reaction is high, owing to the electrostatic repulsion created when the amine with its free electron pair approaches the π-electron cloud of the alkene, therefore the use of a catalyst is inevitable.

With regard to intramolecular aminations in aminoalkenes[1] and aminoalkynes[2] the field has undergone a rapid development, and a broad range of main group and transition-metal catalysts are known to successfully transform a multitude of substrates into desired products. Intermolecular hydroaminations[1,3] are developed to a much lesser extent and the hydroamination of the simplest olefin (ethylene) has been a research focus of continuing interest. The catalytic hydroamination of ethylene with secondary amines in the presence of rhodium and iridium compounds was reported in 1971,[4] and in subsequent years a variety of catalysts based on these two metals were identified.[5] The stochiometric addition of secondary amines to coordinated ethylene in platinum compounds was reported between 1968 and 1973,[6] and catalytic variants recently employed platinum salts, such as platinum bromide.[7] The base-catalysed hydroamination of ethylene with diethylamine also has been ex-

[a] Dipl.-Chem. A. Uhe, Dr. M. Hölscher, Prof. Dr. W. Leitner
Institut für Technische und Makromolekulare Chemie
RWTH Aachen University
Worringerweg 1, 52074 Aachen (Germany)
Fax: (+49) 241-8022177
E-mail: hoelscher@itmc.rwth-aachen.de
leitner@itmc.rwth-aachen.de

Supporting information for this article is available on the WWW under http://dx.doi.org/10.1002/chem.201000669.

   

plored.[8] All catalysts found to date for the hydroamination of ethylene suffer from low activities.

An even more challenging reaction is the homogeneously catalysed reaction of ethylene with ammonia yielding ethylamine (serving as a prototypical reaction between $NH_3$ and unactivated linear olefins), which is not known as yet to the best of our knowledge. It would be interesting to achieve this synthetic goal, as there is a considerable academic and industrial interest in synthesising amines from simple unactivated olefins and ammonia under mild conditions.

A variety of computationally based publications has shed light on the possibilities and limitations of different hydroamination catalysts.[9] In the present computational study, we wanted to explore the potential of late transition-metal–pincer complexes with classical and nonclassical hydride centres as possible catalysts for this challenging reaction. The aim of this work is to arrive at a complete catalytic cycle for a catalyst under investigation at a reasonable level of accuracy to enable an initial evaluation of the chances for practical feasibility. In particular we hope to obtain answers to the following questions: a) Is there an appropriate catalyst lead structure (i.e., metal/ligand combination), which allows the calculation of closed catalytic cycles with reasonably low activation barriers? b) Are there any side reactions possible? c) Would these side reactions be preferred kinetically or thermodynamically relative to the main cycle? The questions about the detailed (peripheral) structure of the catalyst's ligand, as well as the influence of solvent effects, is not addressed in this study and postponed for future work.

Pincer complexes meanwhile have proven to be useful for many different catalytic reactions[10] and nonclassical hydrides of late transition-metal–pincer complexes have been under investigation as catalysts in our group and proved to be useful in different catalytic reactions.[11] The nonclassically bound $H_2$ moiety is a good leaving group, that is, for the introduction of ethylene or ammonia. We chose iridium[12] and rhodium[13] compounds of type **A** with synthetically available NCN and PCP pincer ligands 2,5-bis(dimethylaminomethyl)benzene and 2,5-bis(dimethylphosphanylmethyl)benzene, respectively, for the investigation of key hydroamination reaction steps.

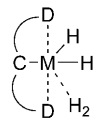

A

## Results and Discussion

For the hydroamination, the following generalised mechanisms were described:[1] Nucleophilic attack at the coordinated alkene (Scheme 2a) or oxidative addition of the nucleophile at the metal complex, followed by olefin insertion into the metal–amide bond (Scheme 2b).

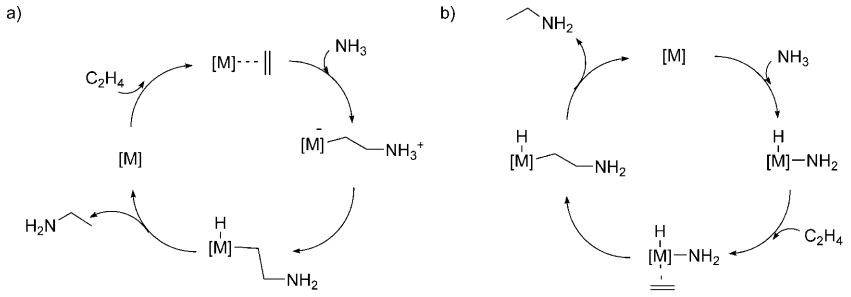

Scheme 2. Hydroamination mechanisms involving the a) activation of the olefin and b) the activation of ammonia.

With catalysts like **A** the classical oxidative addition would not occur in the first place, as there is no available coordination site that allows for the oxidative addition of $NH_3$.[12] However, the replacement of $H_2$ in **A** by $NH_3$ yields a complex, which, in principle, could undergo σ-bond-metathesis to form a metal amide and a new nonclassical hydride. This $H_2$ molecule can be displaced by ethylene, followed by C–N bond formation. In a reductive elimination of ethylamine a complex species without any hydrogen centres present at the metal would be generated opening a path for oxidative addition of $NH_3$. As an alternative to reductive elimination, ethylamine could be liberated by means of σ-bond metathesis with another ammonia molecule. Initially the computations focused on the σ-bond metathesis pathway to evaluate possible metal–ligand combinations. The mechanistic study presented later in this work also takes into account the reductive elimination.

**Comparison of rhodium and iridium complexes with PCP and NCN ligands**: Before the calculation of a complete cycle, the activation barriers of three key reactions were investigated by using catalyst species derived from the parent hydrides $[M(H)_2(H_2)(NCN)]$ and $[M(H)_2(H_2)(PCP)]$ (M = Rh, Ir; NCN = 2,5-bis(dimethylaminomethyl)benzene; PCP = 2,5-bis(dimethylphosphanylmethyl)benzene). It was assumed that these steps presumably will have the highest activation barriers. These steps are: a) N–H bond metathesis of the coordinated $NH_3$, b) C–N bond formation between an amide and coordinated ethylene and c) N–H bond metathesis of the coordinated $NH_3$ under formation of a new amide and the liberation of ethylamine. The results of these calculations are summarised in Table 1 (unless mentioned otherwise we refer to $\Delta G$ and $\Delta G^{\neq}$ values throughout the text).

  

Table 1. Activation enthalpies $\Delta H^{\#}$ and Gibbs free activation barriers $\Delta G^{\#}$ (in italics; all in kcal mol$^{-1}$) for selected key transformations in hydroaminations of $C_2H_4$ with $NH_3$ using Rh- and Ir–pincer complexes.

| | 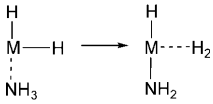 Rh/Ir | 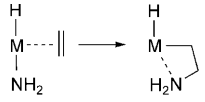 Rh/Ir | 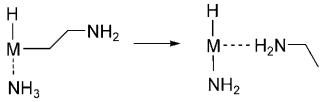 Rh/Ir |
|---|---|---|---|
| 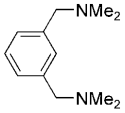 | 14.6, *15.9*/15.6, *16.7* | 22.8, *22.1*/26.0, *25.2* | 11.8, *14.0*/12.3, *13.9* |
| 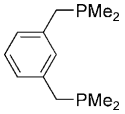 | 24.2, *25.3*/25.1, *26.1* | 22.2, *21.3*/24.6, *23.8* | 18.0, *19.7*/18.7, *20.7* |

We also investigated the outer-sphere attack of $NH_3$ at the coordinated olefin. Despite several attempts for all Rh and Ir complexes studied, it was not possible to locate a transition state for the nucleophilic outer-sphere attack of ammonia at coordinated ethylene. For the [Rh(NCN)] system the outer-sphere attack was studied in more detail. The results are summarised briefly and more details are given in the Supporting Information. Attempts to localise the transition states for the attack of $NH_3$ at an ethylene molecule, which mainly bonds to the rhodium centre with one carbon atom only, while the other carbon atom is bent away from the complex and is being attacked by $NH_3$, were unsuccessful. In the next step we attempted to localise a transition state for $NH_3$ attacking the coordinated ethylene and simultaneously breaking one NH bond, with the hydrogen centre being transferred to the classical hydride centre present at the metal. In this way a nonclassical $H_2$ unit is generated. It was possible to localise such transition states, however the activation barriers amount to 39.9 and 36.7 kcal mol$^{-1}$. These barriers are much higher than all other barriers found, and therefore such pathways will be kinetically less preferred to the many other local pathways (vide infra). Accordingly the outer-sphere mechanism does not seem to operate for such complexes and it was not studied further.

Transition states for C–N bond formation and for N–H bond metathesis, however, were found and the according free activation barriers and Gibbs free activation barriers could be calculated. For the [Rh(NCN)] system the activation barriers of the metathetic N–H cleavage of $NH_3$ coordinated at the metal ($\Delta G^{\neq} = 15.9$ kcal mol$^{-1}$) and the metathetic reaction of $NH_3$ with the metal-bound amine ($\Delta G^{\neq} = 14.0$ kcal mol$^{-1}$) do not differ significantly from the corresponding iridium system (16.7 and 13.9 kcal mol$^{-1}$, respectively). However, for both metals the PCP ligand leads to Gibbs free activation barriers, which are significantly higher. In particular, the activation barrier for the N–H bond cleavage, during the formation of the metal amide and the nonclassical $H_2$ unit, amounts to 25.3 and 26.1 kcal mol$^{-1}$ for the rhodium and the iridium compound, respectively. With regard to the N–C bond-forming reaction, interestingly the PCP ligand yields a slightly lower activation barrier for the [Rh(PCP)]-system ($\Delta G^{\neq} = 21.3$ kcal mol$^{-1}$), which is the lowest activation barrier for this step. The same activation barrier for the [Rh(NCN)] complex, however, is only 0.8 kcal mol$^{-1}$ higher ($\Delta G^{\neq} = 22.1$ kcal mol$^{-1}$). As the other two reaction barriers for the Rh-NCN ligand were significantly lower when compared to the Rh–PCP ligand, NCN as the ligand was chosen for the elucidation of a complete catalytic cycle. From both $\Delta H^{\neq}$ and $\Delta G^{\neq}$ values shown in Table 1 it can be deduced that regardless of the ligand backbone the iridium compounds yield slightly to significantly larger activation barriers than the rhodium compounds. The most favourable option is the combination of rhodium, as the transition metal centre, with the NCN ligand.

**Generation of the active species 5 and 17 from precatalysts *trans*-1 and *cis*-1**: Initially the activation of precatalyst **1** as the catalyst species was investigated. As transition-metal hydride pincer complexes are known for the dynamic exchange of classical and nonclassical hydrides, the possible isomers of **1** had to be investigated. The calculations show, that both *trans*-**1** and *cis*-**1** are stable minima, with *trans*-**1** 5.0 kcal mol$^{-1}$ more stable than *cis*-**1** (Scheme 3 and Figure 1). A transition state also was located and the Gibbs free activation energy for the reaction from *trans*-**1** to *cis*-**1** is 7.4 kcal mol$^{-1}$ (2.4 kcal mol$^{-1}$ for the backward reaction) was calculated. Accordingly both complexes would be available in an experimental system and $NH_3$ or $C_2H_4$ can displace $H_2$ at both complexes. It will be shown that these two complexes can serve as precatalysts for the generation of two active catalyst species namely the $Rh^{III}$–amido complexes [Rh(NCN)(H)($NH_2$)] (**5**) and [Rh(NCN)($C_2H_5$)($NH_2$)] (**17**). Therefore, we can describe how **5** and **17** are generated. The associated valence bond structures and an energy profile is presented in Scheme 3 and Figure 1, respectively. The catalytic cycles starting with **5** are described subsequently (Scheme 4 and Figure 2). The structures and energy profiles associated with **17** are presented in Scheme 5 and Figure 3, respectively and the side reactions are shown in Scheme 6. The relative energies for all reaction paths are given in Table 2 (for the ball-and-stick representations, as well as the Cartesian coordinates, of all compounds calculated in this work see the Supporting Information).

*Path I*: Starting with the more stable *trans*-**1** the inevitable first step is the replacement of $H_2$ by either $NH_3$ or $C_2H_4$. When ammonia displaces $H_2$ in *trans*-**1** the reaction has a negligible exergonic trend (−0.4 kcal mol$^{-1}$) and leads to **3**,

  

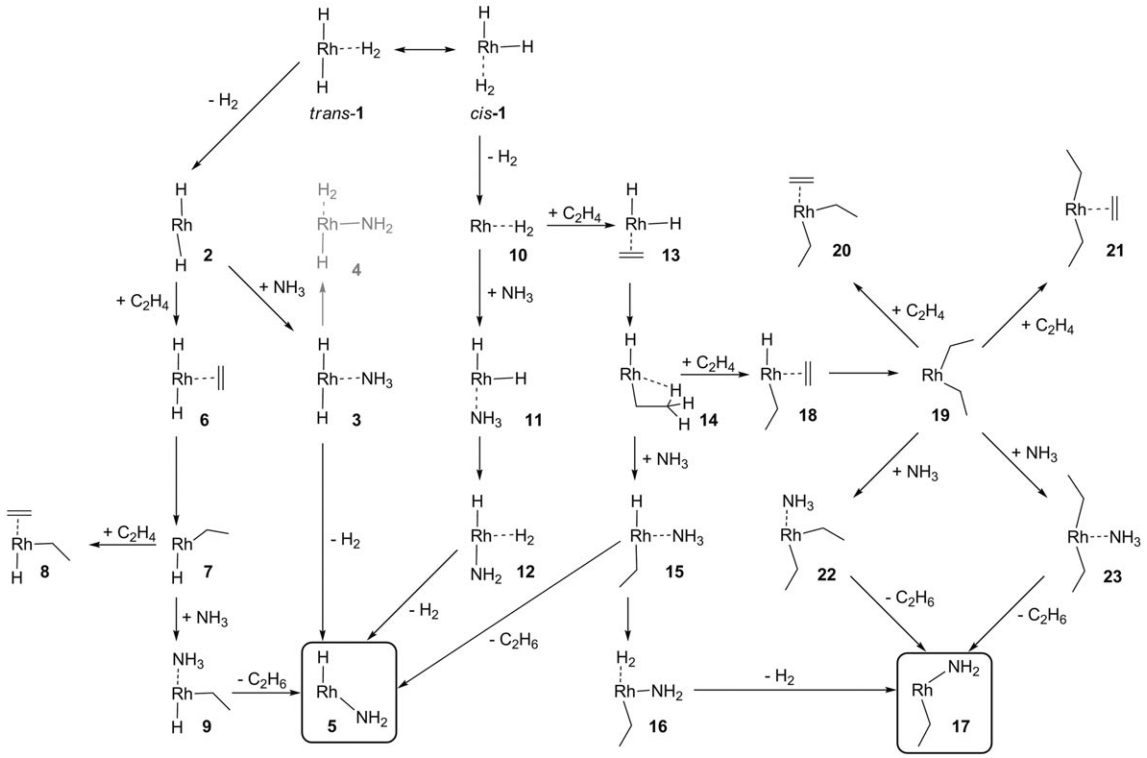


Scheme 3. Valence bond structures for the generation of active catalyst species **5** and **17** using *trans*-**1** and *cis*-**1** as catalyst precursors, respectively. Path I: *trans*-**1**, **2**, **3**, **5**; Path II: *trans*-**1**, **2**, **6**, **7**, **9**, **5**; Path III: *cis*-**1**, **10**, **11**, **12**, **5**; Path IV: *cis*-**1**, **10**, **11**, **13**, **14**, **15**, **5**; Path V: *cis*-**1**, **10**, **13**, **14**, **15**, **16**, **17**; Path VI: *cis*-**1**, **10**, **13**, **14**, **18**, **19**, **22** or **23**, **17**. Structures in grey could not be localised.

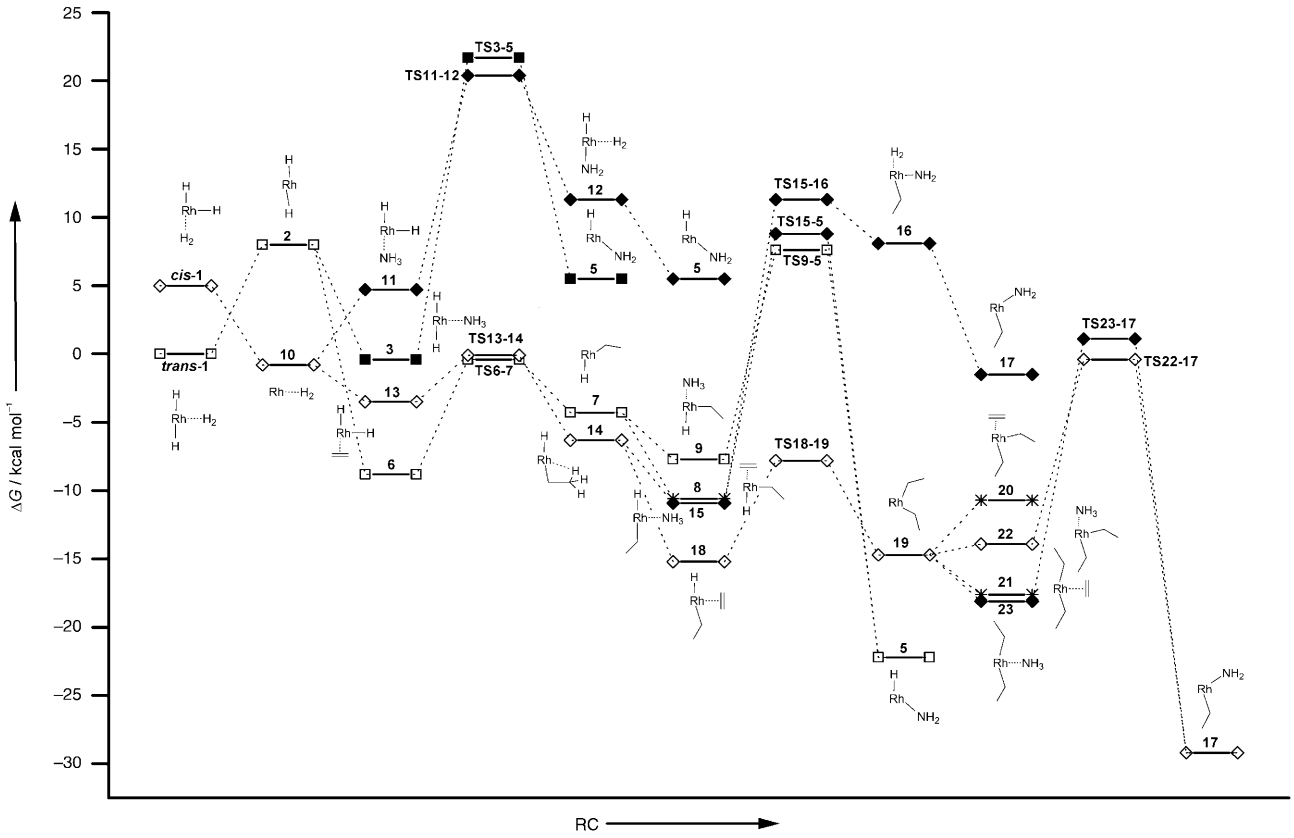


Figure 1. The energy profile for the generation of active catalyst species **5** and **17** using *trans*-**1** and *cis*-**1** as catalyst precursors, respectively ($\Delta G$ in kcal mol$^{-1}$). The pathways starting from *trans*-**1** are depicted with squared symbols (■□), whereas those starting from *cis*-**1** use diamonds (◆◇). The preferred pathways are marked by the respective open symbols (◇□) and dead ends are marked by stars (*).

  

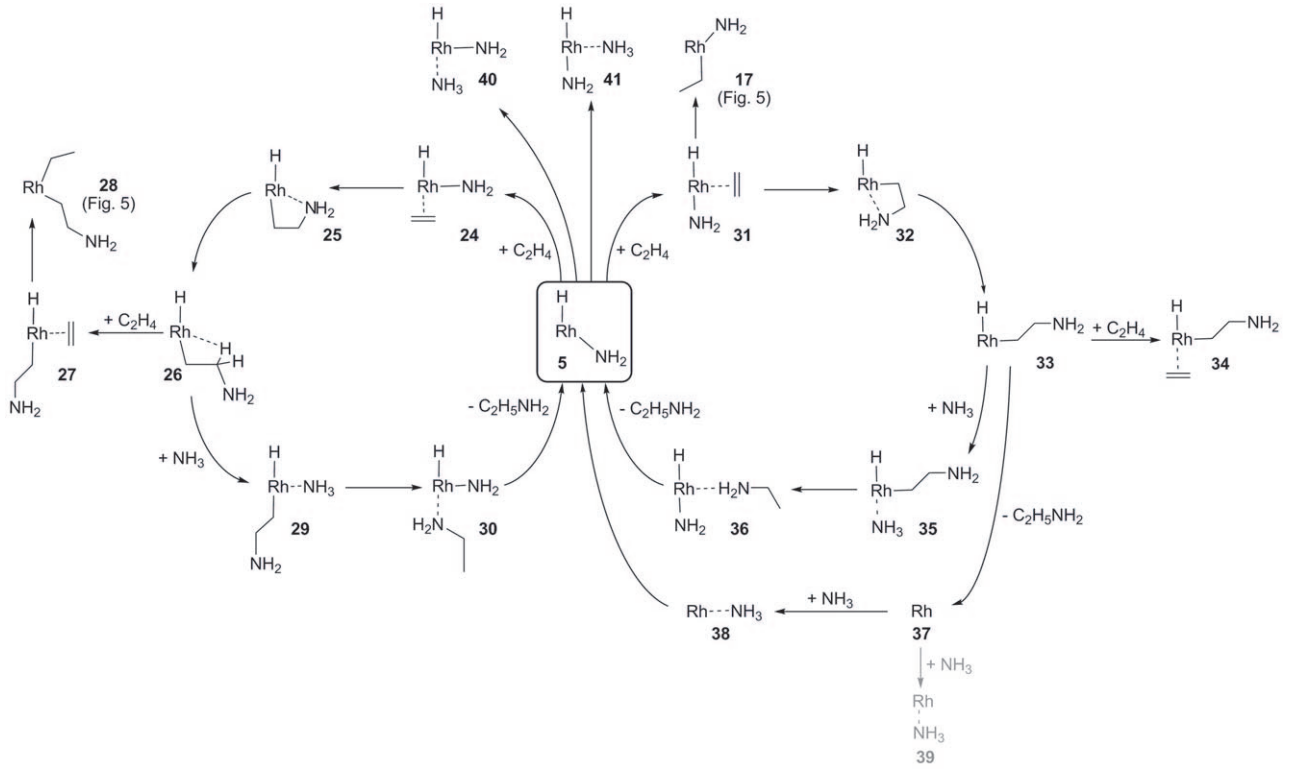


Scheme 4. Reaction pathways using **5** as the active catalyst species. Structures in grey could not be localised.

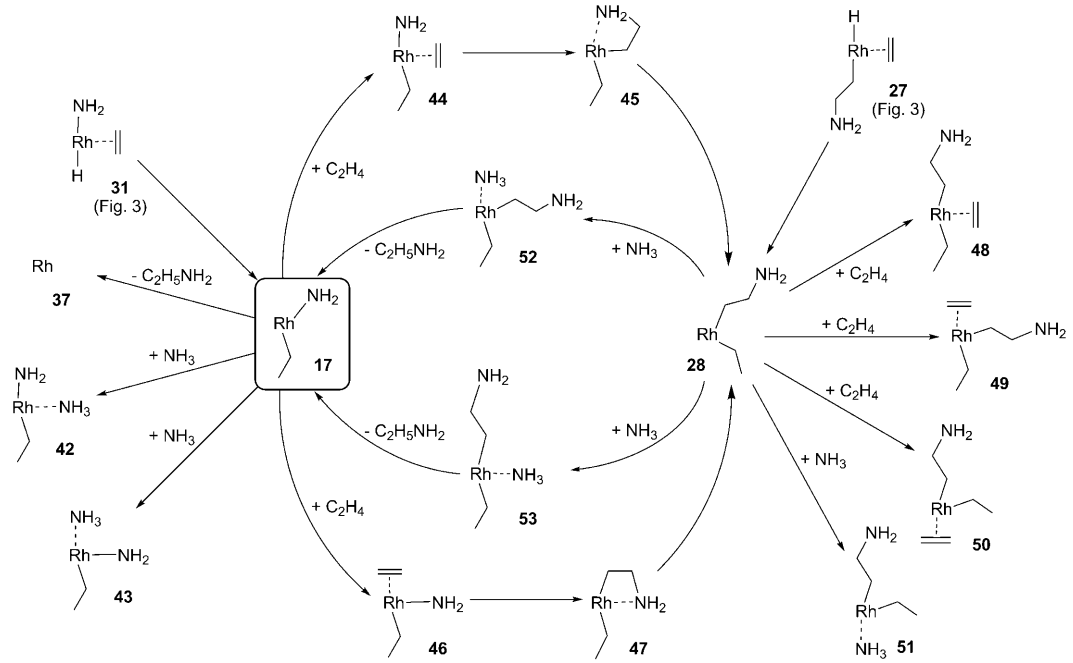


Scheme 5. Reaction pathways obtained with **17** as the active catalyst species.

with **2** being the intermediate classical *trans*-dihydride resulting from the loss of $H_2$ from *trans*-**1**. Complex **2** could be located and it is less stable than *trans*-**1** by 8.0 kcal mol$^{-1}$. In a σ-bond metathesis, the coordinated $NH_3$ in **3** is expected to react to **4**, but it was found that **4** does not exist as a local minimum. Instead the newly formed $H_2$ molecule is dissociating from the complex and the $Rh^{III}$–amide **5** is formed. The activation barrier for the reaction of **3** to **5** is 22.1 kcal mol$^{-1}$, and the sum of the energies of the resulting products **5** and $H_2$ is higher by 4.5 kcal mol$^{-1}$ than the energy of **3**, in-

  

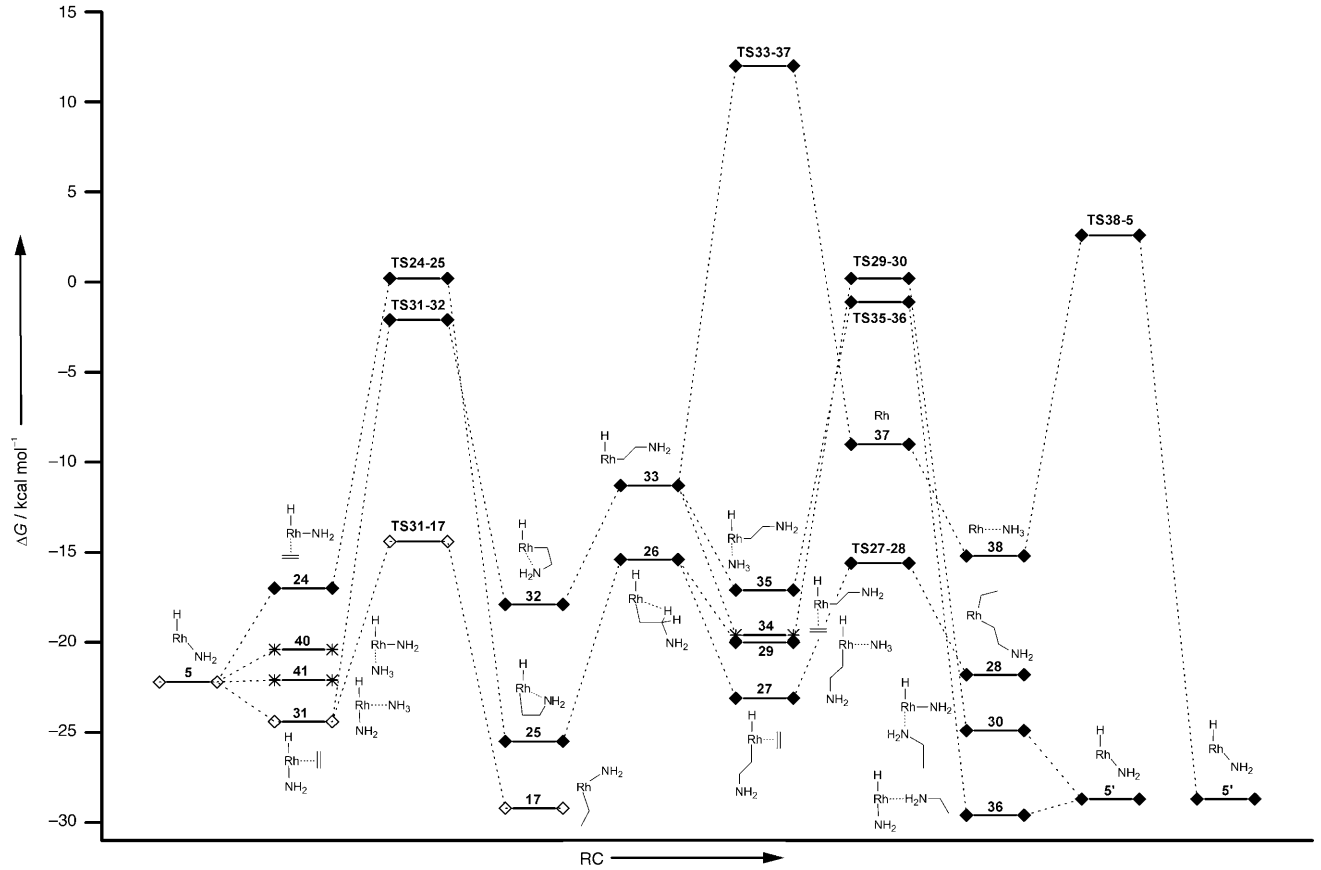


Figure 2. Energy profile for the reaction pathways using **5** as active catalyst species ($\Delta G$ in kcal mol$^{-1}$). The preferred pathway is marked by the open diamonds (◇) and dead ends are marked by stars (*).

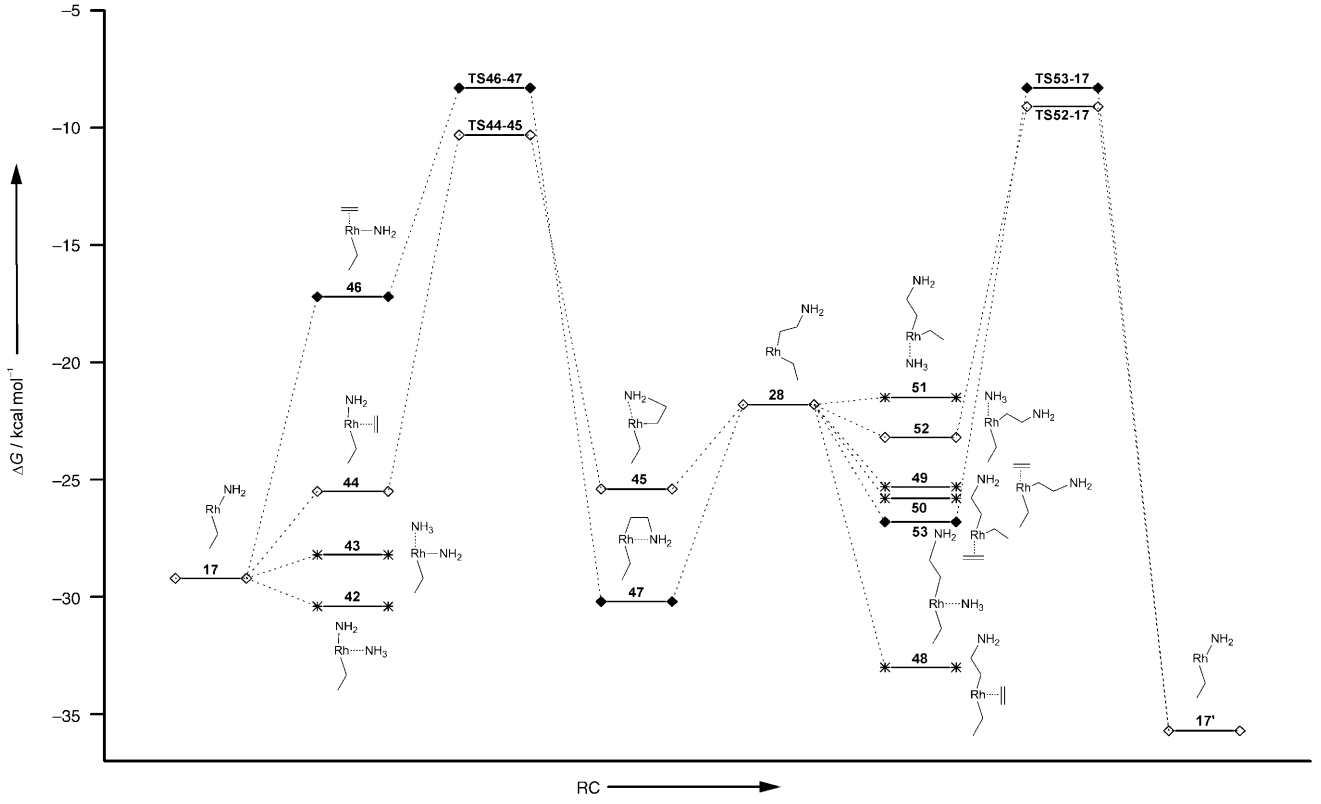


Figure 3. Energy profile for the catalytic cycles using **17** as active catalyst species ($\Delta G$ in kcal mol$^{-1}$). The preferred pathway is marked by the open diamonds (◇) and dead ends are marked by stars (*).

  

Table 2. Relative energies $\Delta G$ of all structures and activation barriers $\Delta G^{\#}$ for all transition states [all in kcal mol$^{-1}$].

| Structure | $\Delta G$ | $\Delta G^{\#}$ | Structure | $\Delta G$ | $\Delta G^{\#}$ | Structure | $\Delta G$ | $\Delta G^{\#}$ |
|---|---|---|---|---|---|---|---|---|
| Scheme 3/Figure 1, Path I | | | Scheme 3/Figure 1, Path VI | | | Scheme 4/Figure 2, reductive elimination | | |
| *trans*-**1** | 0.0 | | *cis*-**1** | 5.0 | | **5** | −22.2 | |
| **2** | 8.0 | | **10** | −0.8 | | **31** | −24.4 | |
| **3** | −0.4 | | **13** | −3.5 | | **TS31-32** | −2.1 | 22.3 |
| **TS3-5** | 21.7 | 22.1 | **TS13-14** | −0.1 | 3.4 | **32** | −17.9 | |
| **5** | 5.5 | | **14** | −6.3 | | **33** | −11.3 | |
| | | | **18** | −15.2 | | **TS33-37** | 12.0 | 23.3 |
| Scheme 3/Figure 1, Path II | | | **TS18-19** | −7.8 | 7.4 | **37** | −9.0 | |
| *trans*-**1** | 0.0 | | **19** | −14.7 | | **38** | −15.2 | |
| **2** | 8.0 | | **20** | −10.7 | | **TS38-5** | 2.6 | 17.8 |
| **6** | −8.8 | | **21** | −17.6 | | **5** | −28.7 | |
| **TS6-7** | −0.4 | 8.4 | **22** | −13.9 | | | | |
| **7** | −4.3 | | **TS22-17** | −0.4 | 13.5 | Scheme 5/Figure 3, top cycle | | |
| **8** | −10.6 | | **23** | −18.1 | | **17** | −29.2 | |
| **9** | −7.7 | | **TS23-17** | 1.1 | 19.2 | **44** | −25.5 | |
| **TS9-5** | 7.6 | 15.3 | **17** | −29.2 | | **TS44-45** | −10.3 | 15.2 |
| **5** | −22.2 | | | | | **45** | −25.4 | |
| | | | Scheme 4/Figure 2, left cycle | | | **28** | −21.8 | |
| Scheme 3/Figure 1, Path III | | | **5** | −22.2 | | **52** | −23.2 | |
| *cis*-**1** | 5.0 | | **40** | −20.4 | | **TS52-17** | −9.1 | 14.1 |
| **10** | −0.8 | | **41** | −22.1 | | **17′** | −35.7 | |
| **11** | 4.7 | | **24** | −17.0 | | | | |
| **TS11-12** | 20.4 | 15.7 | **TS24-25** | 0.2 | 17.2 | Scheme 4/Figure 2, bottom cycle | | |
| **12** | 11.3 | | **25** | −25.5 | | **17** | −29.2 | |
| **5** | 5.5 | | **26** | −15.4 | | **46** | −17.2 | |
| | | | **27** | −23.1 | | **TS46-47** | −8.3 | 8.9 |
| Scheme 3/Figure 1, Path IV | | | **TS27-28** | −15.6 | 7.5 | **47** | −30.2 | |
| *cis*-**1** | 5.0 | | **28** | −21.8 | | **28** | −21.8 | |
| **10** | −0.8 | | **29** | −20.0 | | **53** | −26.8 | |
| **13** | −3.5 | | **TS29-30** | 0.2 | 20.2 | **TS53-17** | −8.3 | 18.5 |
| **TS13-14** | −0.1 | 3.4 | **30** | −24.9 | | **17′** | −35.7 | |
| **14** | −6.3 | | **5** | −28.7 | | | | |
| **15** | −10.9 | | | | | | | |
| **TS15-5** | 8.8 | 19.7 | Scheme 4/Figure 2, right cycle | | | Scheme 4/Figure 2, reductive elimination and dead ends | | |
| **5** | −22.2 | | **5** | −22.2 | | **17** | −29.2 | |
| | | | **31** | −24.4 | | **TS17-37** | 6.5 | 35.7 |
| Scheme 3/Figure 1, Path V | | | **TS31-17** | −14.4 | 10.0 | **37** | −9.0 | |
| *cis*-**1** | 5.0 | | **17** | −29.2 | | **42** | −30.4 | |
| **10** | −0.8 | | **TS31-32** | −2.1 | 22.3 | **43** | −28.2 | |
| **13** | −3.5 | | **32** | −17.9 | | | | |
| **TS13-14** | −0.1 | 3.4 | **33** | −11.3 | | **28** | −21.8 | |
| **14** | −6.3 | | **34** | −19.6 | | **48** | −33.0 | |
| **15** | −10.9 | | **35** | −17.1 | | **49** | −25.1 | |
| **TS15-16** | 11.3 | 22.2 | **TS35-36** | −1.1 | 16.0 | **50** | −25.8 | |
| **16** | 8.1 | | **36** | −29.6 | | **51** | −21.5 | |
| **17** | −1.5 | | **5** | −28.7 | | | | |

dicating that the reaction is endergonic. Although the calculated barrier is relatively high, it may not be prohibitive to generate an active catalyst in a solvent environment upon suitable modification of the ligand periphery. Overall the free reaction enthalpy for the transformation of *trans*-**1** to **5** by means of this route is endergonic by 5.5 kcal mol$^{-1}$.

*Path II*: Instead of displacing $H_2$ in *trans*-**1** with ammonia, the complex can react with ethylene, yielding **6**, which is favoured compared to the reaction of *trans*-**1** with $NH_3$, as **6**/$H_2$ is more stable than *trans*-**1**/$C_2H_4$ by −8.8 kcal mol$^{-1}$. The activation barrier for the insertion of the coordinated olefin into the M–H bond is low enough to be accomplished (8.4 kcal mol$^{-1}$) and the resulting alkyl complex **7** is less stable than **6** by 4.5 kcal mol$^{-1}$. If another $C_2H_4$ molecule coordinates at the free site in **7**, compound **8** is formed and this process liberates −6.3 kcal mol$^{-1}$ of energy, while leading to a dead end of the cycle.[14a] The uptake of $NH_3$ by **7** also is exergonic (−3.4 kcal mol$^{-1}$) yielding **9** and the subsequent σ-bond metathesis to **5** and ethane requires an activation energy of 15.3 kcal mol$^{-1}$ leading to the much more stable **5**/$C_2H_6$ (−14.5 kcal mol$^{-1}$). The whole sequence from *trans*-**1** to **5** is exergonic by −22.2 kcal mol$^{-1}$.

*Paths III and IV*: If $H_2$ is removed from *cis*-**1** the geometry optimisation results in compound **10**, which is a nonclassical $Rh^{I}$-hydride. **10** is more stable than *cis*-**1** by −5.8 kcal mol$^{-1}$ and also more stable than *trans*-**1** by −0.8 kcal mol$^{-1}$. While attempting to synthesise *trans*- or *cis*-**1**, one might instead arrive at **10** as the product, though the energy differences

  

are low enough to be reversed by solvent effects. As with **2**, competitive pathways resulting from either the addition of $NH_3$ or $C_2H_4$ to **10** exist and, accordingly, the analogous routes lead to **5** by Path III: Addition of $NH_3$ (**11**), σ-bond metathesis (**12**), and $H_2$-elimination (**5**) and Path IV: addition of $C_2H_4$ (**13**), insertion into the Rh–H bond (**14**), addition of $NH_3$ (**15**), and σ-bond metathesis with concomitant elimination of ethane (**5**).

The loss of hydrogen is the first step in Paths I to IV. This step can be considered irreversible, because in an experimental system the concentration of the released hydrogen will be much lower than the concentration of the reactants ethylene and ammonia. So despite the fact that *cis*-**1** and *trans*-**1** can be interconverted the first step decides if reaction Paths I and II (loss of hydrogen from *trans*-**1**) or Paths III and IV (loss of hydrogen from *cis*-**1**) can be accessed. As all four paths include activation barriers that are higher than the activation barrier for interconverting *cis*-**1** and *trans*-**1**, a temperature controlled discrimination between the loss of hydrogen from *cis*-**1** or *trans*-**1** is not possible and both compounds will be actively participating. In the case of loss of hydrogen from *trans*-**1** one has to compare Paths I and II. The intermediates of Path II (**6** $-8.8\,kcal\,mol^{-1}$, **7** $-4.3\,kcal\,mol^{-1}$, **9** $-7.7\,kcal\,mol^{-1}$) are more stable than those of Path I (**3** $-0.4\,kcal\,mol^{-1}$) and also the activation barriers of Path II (**TS6–7** $8.4\,kcal\,mol^{-1}$, **TS9–5** 15.3 kcal $mol^{-1}$) are lower than those of Path I (**TS3–5** 22.1 kcal $mol^{-1}$). This shows Path II to be clearly kinetically preferred. In the case of loss of hydrogen from *cis*-**1**, however, there are further pathways competing with Paths III and IV.

*Path V*: For example, as an alternative, **15** can undergo a σ-bond metathesis with the metal bound hydride centre, resulting in the formation of the amido species **16**. The activation barrier for this reaction amounts to 22.2 kcal $mol^{-1}$. The removal of $H_2$ from **16** is exergonic by $-9.6\,kcal\,mol^{-1}$ and leads to the Rh-amido-alkyl complex **17**. However, the barrier for **TS15–16** is higher than that of **TS15–5** (19.7 kcal $mol^{-1}$) rendering Path IV more viable than Path V.

*Path VI*: Furthermore, **14** can add one more ethylene molecule leading to **18** in an exergonic step ($-8.9\,kcal\,mol^{-1}$) and **18** can subsequently react to **19** by insertion of the coordinated $C_2H_4$ into the Rh–H bond. The activation barrier amounts to $7.4\,kcal\,mol^{-1}$ and **19** has practically the same stability as **18**. Intermediate **19** has a trigonal bipyramidal structure and it can be imagined that one of its ethyl ligands rearranges to a *trans*- or to a *cis*-position relative to the pincer backbone. This would create available coordination sites, which can be occupied by $C_2H_4$ or by $NH_3$. If $C_2H_4$ is added, two dead-ends are created resulting in complexes **20** and **21**, which are less stable (**20**) and more stable (**21**) than **19** by 4.0 and $-2.9\,kcal\,mol^{-1}$, respectively.[14a] However, the addition of $NH_3$ resulting in **22** and **23** is either practically thermoneutral (**22**) or exergonic ($-3.4\,kcal\,mol^{-1}$, **23**) and more importantly enables **22** and **23** to react to **17** through σ-bond-metathesis and generation of ethane. The activation barrier for this step is $13.5\,kcal\,mol^{-1}$ for the transformation of **22** to **17** and $19.2\,kcal\,mol^{-1}$ for the reaction of **23** to **17**. The formation of **17** is exergonic and puts the complex on the lowest point of the energy profile as yet ($-28.2$ kcal $mol^{-1}$). The reaction sequence *cis*-**1**, **10**, **13**, **14**, **18**, **19**, **22**, **17** of Path VI has the lowest activation barriers (**TS13–14** $3.4\,kcal\,mol^{-1}$, **TS18–19** $7.4\,kcal\,mol^{-1}$, **TS22–17** 13.5 kcal $mol^{-1}$) compared to Paths III (**TS11–15** $15.7\,kcal\,mol^{-1}$) and IV (**TS13–14** $3.4\,kcal\,mol^{-1}$, **TS15–5** $19.7\,kcal\,mol^{-1}$). Additionally, the intermediates of Path VI are more stable than those of the other paths, so for the case of hydrogen loss of *cis*-**1** the active species **17** will be formed. In summary, the analysis of all paths investigated shows that the system can either operate through Path II leading to **5** or the alternative Path VI to generate **17**.

As **5** and **17** are the entry points into the catalytic cycles it is important to discuss the structures of these complexes in some detail. The hydride centre in **5** and the ethyl ligand in **17** adopt a *cis*-position to the pincer backbone. The H-Rh-C angle between the hydridic H and the aromatic C atom of the pincer ligand binding to Rh in **5** is 73.1°, whereas an angle of 84.7° was determined for the C-Rh-C angle in **17**. The $NH_2$ ligand neither adopts a *cis*- nor a *trans*-position to the pincer backbone. Instead it resides in an intermediate position. The C-Rh-N angle in **5** amounts to 145.1°, whereas the corresponding angle in **17** has a value of 144.1°. Accordingly the Rh centre can be described as a strongly distorted trigonal bipyramid. The structural consequences of the addition of $NH_3$ or $C_2H_4$ to either **5** or **17** stem from the fact that the $NH_2$ group can move to the *cis*- or to the *trans*-position, indicating that the formation of a variety of complexes is possible, which can react in alternative pathways.

**Cycles with 5 as the active catalyst species**: If $C_2H_4$ is added *cis* to the backbone of **5** then complex **24** is generated. This reaction is endergonic by $5.2\,kcal\,mol^{-1}$. The subsequent formation of the C–N bond generates complex **25** with an activation barrier of $17.2\,kcal\,mol^{-1}$, although **25** is more stable than **24** by $-8.5\,kcal\,mol^{-1}$. Either **25** collides directly with $C_2H_4$ or $NH_3$ or it might rearrange to the less stable **26**, with an agostic C–H interaction to the metal. If $C_2H_4$ is added then complex **27** is formed, which can react to **28** via a low-lying transition state ($\Delta G^{\neq} = 7.5\,kcal\,mol^{-1}$). If this path is chosen, the system enters one of the cycles in which **17** is the active catalyst species. The reaction of **28** to other products is described there. If instead $NH_3$ is added to **26** then the reaction results in the formation of **29**, which can undergo σ-bond metathesis to ethylamine and **5**, however, before ethylamine is cleaved off from the complex, compound **30** might form as an intermediate. The activation barrier for the reaction from **29** to **30** amounts to $20.2\,kcal\,mol^{-1}$. Interestingly the removal of ethylamine from **30** forming **5** is exergonic by $-3.8\,kcal\,mol^{-1}$.

The *trans*-addition of $C_2H_4$ to **5** generates **31**, which is an isomer of **24** the positions of the $C_2H_4$- and $NH_2$-ligand being exchanged. The cycle **5**, **31**, **32**, **33**, **35**, **36**, **5′** resembles the cycle discussed above for the *cis*-addition of $C_2H_4$ and as

  

the energetic profile of this cycle does not differ substantially from the cycle **5**, **24**, **25**, **26**, **29**, **30**, **5′** it will not be discussed in detail. However, it should be noted that **33**, instead of adding $NH_3$, could instead undergo a reductive elimination of ethylamine to generate the $Rh^I$ complex **37**, which, after *trans*-addition of $NH_3$ (**38**), could react in an oxidative addition to **5** and in this way close the cycle ($\Delta G^{\neq} = 17.8\ kcal\,mol^{-1}$). This subcycle is not favoured, as the activation energy for the reaction of **33** to **37** is relatively high ($\Delta G^{\neq} = 23.3\ kcal\,mol^{-1}$) and, furthermore, **33** is already relatively rich in energy. The *cis*-addition of $NH_3$ to **37** leading to **39** is not possible, as all attempts to optimise this structure led to **38**.

The addition of $NH_3$ to **5** *cis* or *trans* to the pincer backbone also is possible leading to **40** and **41**, which are less stable than **5**/$NH_3$ by 0.1 $kcal\,mol^{-1}$ and 1.8 $kcal\,mol^{-1}$, respectively. These structures are dead ends, which will react back to **5** releasing the ammonia ligand.[14b]

More important is the fact that **31** instead of reacting to **32** could also undergo insertion of the coordinated $C_2H_4$ molecule into the Rh–H bond and, in this way, react to **17**. This pathway has an activation barrier of 10.0 $kcal\,mol^{-1}$ and is competitive with the first step of the catalytic cycles presented up to this point. As the relative energy of **TS31–17** is lower than the relative energy of **TS31–32** and **TS24–25** by 12.3 $kcal\,mol^{-1}$ and 14.6 $kcal\,mol^{-1}$, respectively, it is clear that **5** will not act as a catalyst, but will rather form **17**. Accordingly it does not matter, if one generates **5** or **17** on the way from *cis*-**1** or *trans*-**1**, as one will end up with **17**, even if **5** is generated first.

**Cycles with 17 as the active catalyst species**: As with **5**, a variety of pathways were calculated for the reaction of **17** with $NH_3$ or $C_2H_4$. Ammonia can add *trans* or *cis* to the pincer backbone, resulting in complexes **42** and **43** as dead ends for the cycle.[14b] However, a reductive elimination of ethylamine from **17** could also be possible, resulting in the $Rh^I$ complex **37**, which would enable the cycle discussed above. The activation barrier for the reaction of **17** to **37** is relatively high ($\Delta G^{\neq} = 34.7\ kcal\,mol^{-1}$) and accordingly this pathway would be clearly kinetically disfavoured.

If $C_2H_4$ adds to **17**, both *cis*- and *trans*-attack to **17** will eventually lead to the formation of complex **28**, which structurally resembles complex **19**, as the coordination geometry about the Rh centre can be described as trigonal bipyramidal. The *trans*-addition of $C_2H_4$ to **17** is energetically favoured, relative to the *cis*-addition, as the *trans*-product **44** is less stable than **17**/$C_2H_4$ by 2.7 $kcal\,mol^{-1}$, whereas the *cis*-product **46** is less stable than **17**/$C_2H_4$ by 11.0 $kcal\,mol^{-1}$. Complex **44** undergoes C–N bond formation yielding **45**. This reaction step has an activation barrier of 15.2 $kcal\,mol^{-1}$, whereas isomer **46** reacts to **47** with an activation barrier of 8.9 $kcal\,mol^{-1}$. In **45** and in **47** the N atom of the amine group coordinates to the metal centre. However this coordination can be broken and results in the formation of **28** in both cases. Complex **28** is less stable than **45** and **47** by 3.6 and 8.4 $kcal\,mol^{-1}$, respectively.

As **28** carries an ethyl and an aminoethyl ligand three isomers exist each for the addition of $NH_3$ or $C_2H_4$. If $C_2H_4$ is added to **28**, compounds **48**, **49** and **50** are formed, whereas the addition of $NH_3$ yields **51**, **52** and **53**. At this stage we regard **48**, **49** and **50** as dead ends that can easily react back to **28**.[14a] Complex **51** could theoretically react in a σ-bond metathesis to $[(NCN)Rh(NH_2)(CH_2CH_2NH_2)]$ with a structure analogous to **17**, simply with the ethyl ligand at the metal centre replaced by an aminoethyl ligand. As there is no obvious reason to assume the amino group of this aminoethyl ligand to change the electronic conditions at the metal centre (the $NH_2$ rest being remote from the complex) it is plausible to assume that such a complex is an active catalyst for the generation of ethylamine following the cycles that are possible for **17**. Therefore, no transition state for the σ-bond metathesis of **51** to $[(NCN)Rh(NH_2)(CH_2CH_2NH_2)]$ was calculated.

The reaction of **28** with $NH_3$ via **52** or **53** (*trans* versus *cis*-addition, respectively) proceeds by liberation of ethylamine to form **17**. The path via **52** is favoured kinetically, as the activation barrier is 14.1 $kcal\,mol^{-1}$, whereas the activation barrier for the path leading from **53** to **17** is 18.5 $kcal\,mol^{-1}$.

Summarising the information obtained by investigating the cycles possible for catalyst **17**, it is important to note that one pathway (**17**, **44**, **45**, **28**, **52**, **17**) could be derived that enables ethylamine formation via transition states **TS44–45** and **TS52–17**, which have activation barriers (15.2 and 14.1 $kcal\,mol^{-1}$, respectively) low enough for the reaction to proceed. Interestingly, it is not necessary to synthesise compounds *trans*-**1**, *cis*-**1** or **10**, instead the synthesis of **17** would yield an active catalyst without the need for preactivation.

To estimate the reaction rate expected for an experimental setup starting with **17**, as the active catalyst, the presence of low lying intermediates like **42**, **47** and **48** had to be taken into account. To get a reasonable estimate of the turnover frequency (TOF) it is convenient to use the energetic span model[15a–d] for the evaluation of the reaction sequence **17**-**44**-**45**-**28**-**52**-**17′** (for details see the Supporting Information). If **42**, **47** and **48** are considered as possible species (reaction temperature of 50 °C, reactant concentrations of 0.1 $mol\,L^{-1}$) then the energetic span model predicts a TOF of 1 $h^{-1}$ (a value of 6 $h^{-1}$ was calculated, when the dormant species are not taken into account). Accordingly, in laboratory scale reactions, product formation should be observed under mild conditions after prolonged reaction times. Optimising the temperature, as well as the reactant concentrations, should result in an increase of the TOF.

**Oligomerisation/polymerisation**: It would extend beyond the scope of this work to study oligomerisation/polymerisation in detail, especially as Rhodium is not a classical polymerisation metal. However, it is informative to realise that a number of isomers (**8**, **18**, **20**, **21**, **27**, **34**, **44**, **48**, **49**, **50**), in principal, could undergo insertion of coordinated $C_2H_4$ into the Rh–C bond, that is an ethyl or ethylamine ligand forming a new Rh–C bond with an elongated carbon

  

chain. To elucidate whether oligomerisation processes would be possible and competitive, we chose complexes **18**, **21** and **44** as examples to localise transition states for the first step of such a reaction sequence (Scheme 6a). The formation of a new C–C bond is possible in all three cases, as all transition states could be located. Although for the reaction of **18** and **44** the activation barriers amount to values of 26.0 and 27.1 kcal mol$^{-1}$, the reaction barrier is lower for **21** (23.4 kcal mol$^{-1}$). As a result, the oligomerisation processes starting with **21** cannot be ruled out at this stage, whereas **18** and **44** are less prone to start oligomerisations. However, it should be noted that the most preferred reaction pathway, which leads to the active species **17**, has a maximum barrier of 13.5 kcal mol$^{-1}$. Furthermore the most preferred catalytic cycle generating ethylamine from **17** has a maximum activation barrier of 15.2 kcal mol$^{-1}$. Taking these barriers into account, the only intermediate for which oligomerisation is competitive to the hydroamination is **48**, as it is much more stable (−9.8 kcal mol$^{-1}$) than intermediate **52**, which continues the hydroamination cycle. Therefore, the barrier for C–C bond formation using **48** was also investigated (Scheme 6a). The relative energy of the two possible transition states leading to insertion into the Rh–C bond **TS48–59** and **TS48–60** is lower and higher than that of **TS52–17** by −0.3 and 0.4 kcal mol$^{-1}$, respectively. However, these energy differences are too small, to discriminate between each of them distinctively. As a result, longer chain amines should also be expected as products.

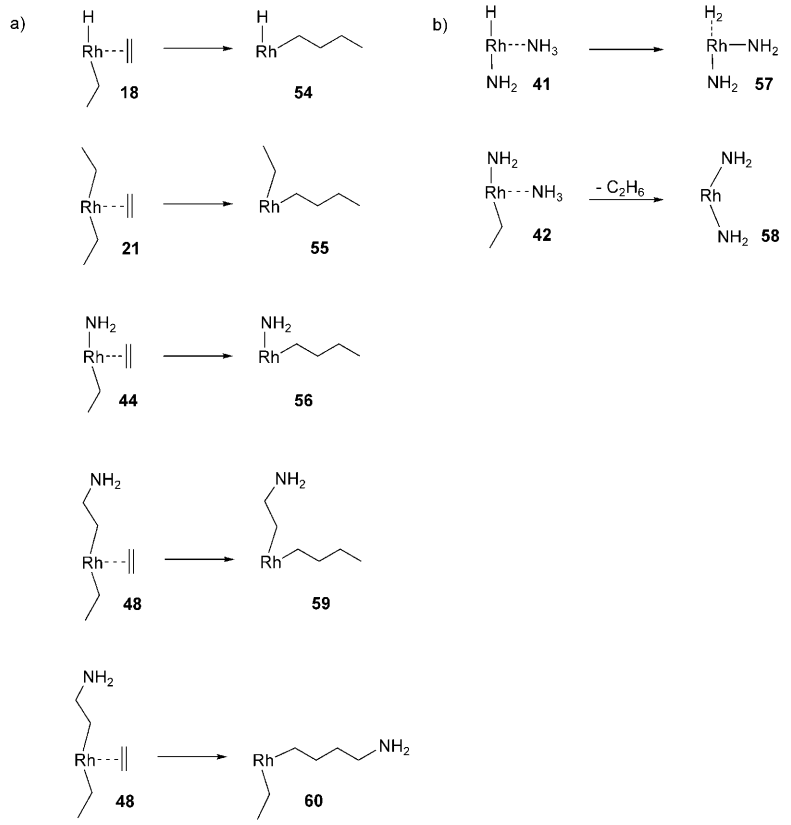


Scheme 6. a) Selection of intermediates available as potential starting points for oligomerisation processes; b) Potential formation of diamides.

**Diamide formation**: In principle, Rh$^{III}$-diamides also could be generated from both **5** and **17**. For instance **5** and **17** can undergo *trans*-additions of $NH_3$ leading to **41** and **42**, respectively. Complex **41** can react with diamide **57** through σ-bond metathesis and subsequently form complex **58** by loss of the nonclassical $H_2$ moiety (Scheme 6b). The activation barrier for the reaction **41** to **57** amounts to 29.6 kcal mol$^{-1}$. Compound **57** is less stable than **41** by 27.3 kcal mol$^{-1}$. The cleavage of $H_2$ from **57** is exergonic, as **58** is more stable than **57** by −11.2 kcal mol$^{-1}$. Alternatively, in a σ-bond metathesis, **42** can react to form **58** and ethane, with an activation barrier of 26.3 kcal mol$^{-1}$. Both barriers are significantly higher than the ones found for the generation of **5** and **17**, and these barriers also are much higher than those of the preferred catalytic cycle. Therefore, it is unlikely that in an experimental system that the formation of diamides would be observed.

## Conclusion

In this work we have computationally investigated the catalytic hydroamination of ethylene with ammonia in the presence of rhodium and iridium centres ligated by NCN and PCP pincer ligands. Initially, in a screening process the activation barriers of three key reaction steps with these complexes were investigated. These key steps were deduced from an analysis of potentially operative reaction mechanisms. As a result, the most promising metal/ligand-combination comprises rhodium, as the catalytically active centre, in combination with the NCN ligand (NCN = 2,5-bis(dimethylaminomethyl)benzene). Complexes of this kind proved to undergo two key transformations with lower barriers relative to the otherwise analogous phosphane system. For the third key step the activation barriers were similar for the rhodium complexes derived with both ligands. The iridium complexes in most cases show slightly to moderately higher activation barriers. As the highest activation barrier found

  

for the rhodium catalyst with the NCN ligand amounted to 22.1 kcal mol$^{-1}$, it was investigated whether active catalyst species and closed catalytic cycles can be derived computationally starting with hypothetical hydride [Rh(NCN)(H)$_2$(H$_2$)] (**1**), in which the nonclassical $H_2$ unit can reside in *cis*- or in *trans*-position relative to the pincer backbone.

Both *trans*-**1** and *cis*-**1** are precatalysts, which enable the formation of the two different active catalysts [Rh(NCN)(H)(NH$_2$)] (**5**) and [Rh(NCN)(C$_2$H$_5$)(NH$_2$)] (**17**). With these two catalysts closed catalytic cycles were calculated with initial activation of either ammonia or ethylene. From the analysis of the different pathways in which the active catalyst species are generated it follows that *cis*-**1** and *trans*-**1** are both actively participating. Starting with *trans*-**1** the reactions lead to **5** and there are two Paths (I and II) of which Path II is clearly favoured. Starting with *cis*-**1** the activation Paths (III to VI) lead to **5** and **17**. Path VI is preferred over Paths III to V.

Upon inspection of the catalytic cycles available with **5** as the catalyst, it turned out that the most preferred pathway would not result in a catalytic cycle, instead complex **17** would be obtained. Among the catalytic cycles possible with **17** one cycle is preferred kinetically. This cycle leads via **44**, **45**, **28**, and **52** to **17′** and ethylamine. In this cycle the maximum activation barrier was calculated to be 15.2 kcal mol$^{-1}$ (**TS44–45**), accordingly this cycle has barriers clearly low enough for a gas phase reaction to be put into practice. Low lying dormant species were identified and according to their relative heights on the hyper surface they will decrease the reaction rate without suppressing the reaction completely.

One of the most interesting results of this study is the fact that neither **1** nor **5** need to be made inevitably. Instead one can directly synthesise **17** as this complex is an active catalyst and it is the one which enables product formation most easily.

We also investigated the relevance of possible side reactions, that is, the entry point to an ethylene oligomerisation or polymerisation and the formation of rhodium-diamide complexes. The corresponding transition states for oligomerisation could be located, which are partly competitive with hydroamination. Accordingly concomitant formation of products with elongated carbon chains should also be expected. The formation of diamides is clearly disfavoured, which suggests these compounds not to be formed in an experimental system.

## Computational Details

Calculations in this work were carried out by using the Turbomole 5.10 program.[16] In the initial screening process of rhodium and iridium complexes the def2-SVP[17] basis set was used for all elements together with the associated ECP for the metal centres, whereas for the calculation of the complete catalytic cycle with the [Rh(NCN)(H$_2$)(H)$_2$] complexes the def2-TZVP[17] basis set was used (together with the associated ECP for Rh). The calculations were performed by using the PBE[18] functional augmented with Grimme's[19] dispersion correction and using the RI-approximation (RI-PBE-D). The nature of all stationary points located was verified by frequency calculations proving the presence of local minima ($i=0$) or transition states ($i=1$). Free enthalpies and Gibb's free energies reported include zero point energy corrections as well as thermal corrections for $T=298.15$ K and $p=1$ bar. Tables listing the energies obtained are included in the supporting information as well as Cartesian coordinates of all compounds. In the main text we refer to $\Delta G$ values unless noted otherwise.

## Acknowledgements

This work was supported by the German–Isreal-Coorporation Project (DIP G7.1). We are grateful for the generous allocation of computation time by the Rechen- und Kommunikationszentrum of RWTH Aachen University.

[1] a) T. E. Müller, K. C. Hultzsch, M. Yus, F. Foubelo, M. Tada, *Chem. Rev.* **2008**, *108*, 3795–3892; b) T. E. Müller, M. Beller, *Chem. Rev.* **1998**, *98*, 675–703; c) K. C. Hultzsch, *Org. Biomol. Chem.* **2005**, *3*, 1819–1824; d) K. C. Hultzsch, *Adv. Synth. Catal.* **2005**, *347*, 367–391; e) S. Hong, T. J. Marks, *Acc. Chem. Res.* **2004**, *37*, 673–686; f) J. J. Brunet, D. Neibecker in *Catalytic Heterofunctionalizsation* (Eds.: A. Togni, H. Grützmacher), Wiley-VCH, Weinheim, **2001**, pp. 91–141.

[2] a) F. Alonso, I. P. Beletskaya, M. Yus, *Chem. Rev.* **2004**, *104*, 3079–3159; b) S. Doye, *Synlett* **2004**, 1653–1672; c) F. Pohlki, A. Heutling, I. Bytschkov, T. Hotoopp. S. Doye, *Synlett* **2002**, 0799–0801.

[3] a) R. Severin, S. Doye, *Chem. Soc. Rev.* **2007**, *36*, 1407–1420; b) F. Pohlki, S. Doye, *Chem. Soc. Rev.* **2003**, *32*, 104.

[4] D. R. Coulson, *Tetrahedron Lett.* **1971**, *12*, 429–430.

[5] a) J. J. Brunet, G. Commenges, D. Neibecker, K. Philippot, *J. Organomet. Chem.* **1994**, *469*, 221–228; b) J. J. Brunet, D. Neibecker, K. Pilippot, *J. Chem. Soc. Chem. Commun.* **1992**, 1215–1216; c) S. E. Diamond, A. Szalkiewicz, F. Mares, *J. Am. Chem. Soc.* **1979**, *101*, 490–491; d) S. E. Diamond, F. Mares, A. Szalkiewicz, *Fundam. Res. Homogeneous Catal.* **1979**, *3*, 345–358; e) A. L. Casalnuovo, J. C. Calabrese, D. Milstein, *J. Am. Chem. Soc.* **1988**, *110*, 6738–6744.

[6] a) A. Panunzi, R. Palumbo, A. De Renzi, G. Paiaro, *Chim. Ind.* **1968**, *50*, 924–925; b) A. Panunzi, A. De Renzi, R. Palumbo, G. Paiaro, *J. Am. Chem. Soc.* **1969**, *91*, 924–925; c) A. Panunzi, A. De Renzi, G. Paiaro, *J. Am. Chem. Soc.* **1970**, *92*, 3488–3489; d) E. Benedetti, A. De Renzi, G. Paiaro, A. Panunzi, C. Pedone, *Gazz. Chim. Ital.* **1972**, *102*, 744–754; e) V. Romano, G. Paiaro, *Chim. Ind.* **1972**, *54*, 658–659; f) D. Hollings, M. Green, D. V. Claridge, *J. Organomet. Chem.* **1973**, *54*, 399–402.

[7] J. J. Brunet, M. Cadena, N. C. Chu, O. Diallo, K. Jacob, E. Mothes, *Organometallics* **2004**, *23*, 1264–1268.

[8] a) J. Seayad, A. Tillack, C. G. Hartung, M. Beller, *Adv. Synth. Catal.* **2002**, *344*, 795–813; V. Khedkar, A. Tillack, C. Benisch, J.-P. Melder, M. Beller, *J. Mol. Catal. A* **2005**, *241*, 175–183; b) ethylamine can be synthesised from $C_2H_4$ and $NH_3$ by irradiating films of the two compounds on gold in ultra high vacuum at 32 K with low-energy electrons: T. Hamann, E. Böhler, P. Swiderek, *Angew. Chem.* **2009**, *121*, 4715–4718; *Angew. Chem. Int. Ed.* **2009**, *48*, 4643–4645.

[9] a) P. A. Hunt, *Dalton Trans.* **2007**, 1743–1754; H. F. Koch, L. A. Girard, D. M. Roundhill, *Polyhedron* **1999**, *18*, 2275–2279; b) H. M. Senn, P. E. Blöchl, A. Togni, *J. Am. Chem. Soc.* **2000**, *122*, 4098–4107; c) C. A. Tsipis, C. E. Kefalidis, *J. Organomet. Chem.* **2007**, *692*, 5245–5255; d) B. F. Straub, R. G. Bergman, *Angew. Chem.* **2001**, *113*, 4768–4771; *Angew. Chem. Int. Ed.* **2001**, *40*, 4632–4635; e) A. Motta, G. Lanza, I. L. Fragala, T. J. Marks, *Organometallics* **2004**, *23*, 4097–4104; S. Tobisch, *J. Am. Chem. Soc.* **2005**, *127*, 11979–11988; f) S. Tobisch, *Chem. Eur. J.* **2006**, *12*, 2520–2531; g) S. Tobisch, *J. Chem. Soc. Dalton Trans.* **2006**, 4277–4285; h) S. Tobisch, *Chem. Eur. J.* **2007**, *13*, 4884–4894; i) S. Tobisch, *Chem. Eur. J.* **2008**,

  

*14*, 8590–8602; j) C. Müller, R. Koch, S. Doye, *Chem. Eur. J.* **2008**, *14*, 10430–10436.

[10] M. E. van der Boom, D. Milstein, *Chem. Rev.* **2003**, *103*, 1759–1792; A. Vigalok, D. Milstein, *Acc. Chem. Res.* **2001**, *34*, 798–807; B. Rybtchinski, D. Milstein, *Angew. Chem.* **1999**, *111*, 918–932; *Angew. Chem. Int. Ed.* **1999**, *38*, 870–883; M. Q. Slagt, D. A. P. van Zwieten, A. J. C. M. Moerkerk, R. J. M. Klein Gebbink, G. van Koten, *Coord. Chem. Rev.* **2004**, *248*, 2275–2282; M. Albrecht, G. van Koten, *Angew. Chem.* **2001**, *113*, 3866–3898; *Angew. Chem. Int. Ed.* **2001**, *40*, 3750–3781.

[11] a) M. H. G. Prechtl, M. Hölscher, Y. Ben-David, N. Theyssen, D. Milstein, W. Leitner, *Eur. J. Inorg. Chem.* **2008**, 3493–3500; b) M. Hölscher, M. H. G. Prechtl, W. Leitner, *Chem. Eur. J.* **2007**, *13*, 6636–6643; c) M. H. G. Prechtl, M. Hölscher, Y. Ben-David, N. Theyssen, R. Loschen, D. Milstein, W. Leitner, *Angew. Chem.* **2007**, *119*, 2319–2322; *Angew. Chem. Int. Ed.* **2007**, *46*, 2269–2272; d) M. H. G. Prechtl, Y. Ben-David, D. Giunta, S. Busch, Y. Taniguchi, W. Wisniewski, H. Görls, R. J. Mynott, N. Theyssen, D. Milstein, W. Leitner, *Chem. Eur. J.* **2007**, *13*, 1539–1546; e) P. Buskens, D. Giunta, W. Leitner, *Inorg. Chim. Acta* **2004**, *357*, 1969–1974; f) D. Giunta, M. Hölscher, C. W. Lehmann, R. Mynott, C. Wirtz, W. Leitner, *Adv. Synth. Catal.* **2003**, *345*, 1139–1145; g) *The Chemistry of Pincer Compounds* (Eds.: D. Morales-Morales, C. L. Jensen), Elsevier, Amsterdam, **2007**; h) D. Morales-Morales, *Rev. Soc. Quim. Mex.* **2004**, *48*, 338–346.

[12] a) For iridium complexes with aromatic and aliphatic PCP pincer ligands and available coordination sites it was shown that the oxidative addition of ammonia is possible at such complexes and that the aromatic ligand favours the ammonia complex, while the equilibrium is shifted to the oxidative addition product when the aliphatic pincer ligand is used: J. Zhao, A. S. Goldman, J. F. Hartwig, *Science* **2005**, *307*, 1080–1082. In the presence of olefins a hydroamination was not observed: b) the reductive elimination of $NH_3$ from different iridium pincer complexes also was studied: M. Kanzelberger, X. Zhang, T. J. Emge, A. S. Goldman, J. Zhao, C. Incarvito, J. F. Hartwig, *J. Am. Chem. Soc.* **2003**, *125*, 13644–13645.

[13] The NCN ligand has been used successfully for the synthesis of rhodium pincer complexes: a) A. A. H. van der Zeijden, G. van Koten, R. Luijk, K. Vrieze, C. Slob, H. Krabbendam, A. L. Spek, *Inorg. Chem.* **1988**, *27*, 1014–1019; b) A. A. H. van der Zeijden, G. van Koten, J. M. Ernsting, C. J. Elsevier, B Krijnen, C. H. Stam, *J. Chem. Soc. Dalton Trans.* **1989**, 317; c) K. Hiraki, Y. Fuchita, Y. Ohta, J. Tsutsumida, K. I. Hardcastle, *J. Chem. Soc. Dalton Trans.* **1992**, 833; nonclassical rhodium hydride complexes are known and were analysed spectroscopically: d) R. L. Taw, H. Mellows, P. S. White, F. J. Hollander, R. G. Bergman, M. Brookhart, D. M. Heinekey, *J. Am. Chem. Soc.* **2002**, *124*, 5100–5108; e) V. I. Bakhmutov, C. Bianchini, M. Peruzzini, F. Vizza, E. V. Vorontsov, *Inorg. Chem.* **2000**, *39*, 1655–1660; f) W. J. Oldham, Jr., A. S. Hinkle, D. M. Heinekey, *J. Am. Chem. Soc.* **1997**, *119*, 11028–11036.

[14] a) The possibility of ethylene insertion into the Rh–C bond as an entry to oligomerisation/polymerisation of ethylene is discussed at the end of this paper; b) the possibity of diamide formation via σ-bond metathesis is discussed at the end of this paper.

[15] To obtain a reasonable impression of the reaction kinetics one needs to consider not only the highest single activation barrier of a reaction pathway (or cycle) as the only rate determining criterion. It is necessary to evaluate the complete energy profile including seemingly inactive and/or energetically low lying species. In a series of publications by Shaik and Kozuch and also later by Campbell and co-workers the systematic mathematical description was derived. Shaik and Kozuch designated their model as the so-called energetic span model: a) S. Kozuch, S. Shaik, *J. Am. Chem. Soc.* **2006**, *128*, 3355–3365; b) S. Kozuch, S. Shaik, *J. Phys. Chem. A* **2008**, *112*, 6032–6041; c) S. Kozuch, S. E. Lee, S. Shaik, *Organometallics* **2009**, *28*, 1303–1308; d) M. Angels Carvajal, S. Kozuch, S. Shaik, *Organometallics* **2009**, *28*, 3656–3665; e) C. Stegelmann, A. Andreasen, C. T. Campbell, *J. Am. Chem. Soc.* **2009**, *131*, 8077–8082; f) C. Stegelmann, A. Andreasen, C. T. Campbell, *J. Am. Chem. Soc.* **2009**, *131*, 13563; g) J. K. Nørskov, T. Bligaard, J. Kleis, *Science* **2009**, *324*, 1655–1656.

[16] TURBOMOLE: a) R. Ahlrichs, M. Baer, M. Haeser, H. Horn, C. Koelmel, *Chem. Phys. Lett.* **1989**, *162*, 165; b) O. Treutler, R. Ahlrichs, *J. Chem. Phys.* **1995**, *102*, 346; O. Treutler, R. Ahlrichs, *Chem. Phys. Lett.* **1995**, *240*, 283; c) K. Eichkorn, O. Treutler, H. Oehm, M. Haeser, R. Ahlrichs, *Chem. Phys. Lett.* **1995**, *242*, 652; d) K. Eichkorn, F. Weigend, O. Treutler, R. Ahlrichs, *Theor. Chim. Acc.* **1997**, *97*, 119; e) F. Weigend, *Phys. Chem. Chem. Phys.* **2006**, *8*, 1057.

[17] a) F. Weigend, R. Ahlrichs, *Phys. Chem. Chem. Phys.* **2005**, *7*, 3297–3305; b) A. Schaefer, H. Horn, R. Ahlrichs, *J. Chem. Phys.* **1992**, *97*, 2571–2577; c) A. Schaefer, C. Huber, R. Ahlrichs, *J. Chem. Phys.* **1994**, *100*, 5829–5835; d) K. Eichkorn, F. Weigend, O. Treutler, R. Ahlrichs, *Theor. Chim. Acc.* **1997**, *97*, 119–124; e) F. Weigend, F. Furche, R. Ahlrichs, *J. Chem. Phys.* **2003**, *119*, 12753–12762; f) D. Andrae, U. Haeussermann, M. Dolg, H. Stoll, H. Preuss, *Theor. Chim. Acta* **1990**, *77*, 123–141; g) B. Metz, H. Stoll, M. Dolg, *J. Chem. Phys.* **2000**, *113*, 2563–2569.

[18] a) P. A. M. Dirac, *Proc. Royal Soc. A* **1929**, *123*, 714; b) J. C. Slater, *Phys. Rev.* **1951**, *81*, 385; c) J. P. Perdew, Y. Wang, *Phys. Rev. B* **1992**, *45*, 13244; d) J. P. Perdew, K. Burke, M. Ernzerhof, *Phys. Rev. Lett.* **1996**, *77*, 3865.

[19] a) S. Grimme, *J. Comput. Chem.* **2004**, *25*, 1463–1799; b) S. Grimme, *J. Comput. Chem.* **2006**, *27*, 1787–1799.

Received: March 16, 2010
Published online: June 25, 2010

  